

DEVELOPMENT OF A NOVEL  
SCANNING NEAR FIELD  
MICROSCOPE WITH A FACILITY OF  
SIMULTANEOUS SHEAR STRESS  
MEASUREMENT



A thesis submitted towards partial fulfilment of  
BS-MS Dual Degree Programme

by  
AJITH V J

under the guidance of  
DR. SHIVPRASAD PATIL  
ASSOCIATE PROFESSOR

INDIAN INSTITUTE OF SCIENCE EDUCATION AND RESEARCH  
PUNE

# Certificate

This is to certify that this thesis entitled "DEVELOPMENT OF A NOVEL SCANNING NEAR FIELD MICROSCOPE WITH A FACILITY OF SIMULTANEOUS SHEAR STRESS MEASUREMENT" submitted towards the partial fulfilment of the BS-MS dual degree programme at the Indian Institute of Science Education and Research Pune represents original research carried out by "AJITH V J" at "INDIAN INSTITUTE OF SCIENCE EDUCATION AND RESEARCH, PUNE", under the supervision of "DR.SHIVPRASAD PATIL" during the academic year 2014-2015.

Student  
AJITH V J



Supervisor  
DR. SHIVPRASAD  
PATIL



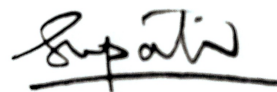
# Declaration

I hereby declare that the matter embodied in the report entitled "DEVELOPMENT OF A NOVEL SCANNING NEAR FIELD MICROSCOPE WITH A FACILITY OF SIMULTANEOUS SHEAR STRESS MEASUREMENT" are the results of the investigations carried out by me at the Department of Physics, Indian Institute of Science Education Research Pune, under the supervision of Dr. Shivprasad Patil and the same has not been submitted elsewhere for any other degree.

Student  
AJITH V J

A handwritten signature in blue ink, appearing to read 'Ajith V J', with a horizontal line underneath.

Supervisor  
DR. SHIVPRASAD  
PATIL

A handwritten signature in black ink, appearing to read 'Shivprasad Patil', with a horizontal line underneath.

# Acknowledgements

First I would like to thank my supervisor Dr. Shivprasad Patil. Thank you for giving me this project. Discussions with him were always encouraging and exciting. So a special thanks goes for him. I would like to thank all the past and present lab members of Nanomechanics lab of IISER Pune, especially Dr. A V R Murthy and Amandeep Sekhon for their guidance and help. My thesis expert Dr. G V Pavan Kumar was always excited about my work. His excitement and the discussions we had with him were a motivation for me. Thank you, Pavan sir. Whenever I had some problems or requirements with electronics or other hardware, I found Nilesh Dumbre resourceful and helpful. Nilesh, thank you very much. I also thank Anil Prathamshetti for helping with FSEM imaging and Prashant Kale for the guidance in electronics. I believe that what I was able to do in this final year was because of the training I received from my semester projects, done in my third and fourth year of BS-MS. A special thanks to Dr. Surjeeth Singh who introduced me to research in my third year. The project I did under him taught me to do disciplined and systematic research. Also I want to thank my seniors Amartya Singh, MD. Noaman and senior PhD, Koushik Karmaker with whom I worked in my first research project. At that time they acted as ideal researchers for me, to see and learn.

I am also extending my gratitude to people at OIM and Texture Lab of IIT Mumbai for providing FIB facility.

I thank all my friends who made my final year a memorable one. Then my parents and my brother...I don't know how to thank them, thank you for the continuous support, trust and prayers.

# Abstract

This project is about building a near-field optical microscope which can simultaneously measure evanescent fields as well as lateral shear forces. Possibility of quantify the lateral shear forces through a special q-plus arrangement using a theoretical model from Manhee et al. and simultaneously measure evanescent field make this instrument unique.

This instrument is built mainly to study water in between two surfaces separated by nanometers. We know very little about this nano-confined water. In-order to get a clear molecular picture of confined water we can look at the diffusion coefficient of a particle through it. By measuring the intensity fluctuations of the light from a fluorescent molecule in this confined water, we can measure it's diffusion coefficient. This instrument can do such a measurement along with measuring mechanical shear response forces.

The instrument uses a tuning fork as the force sensor and a special optical probe for sensing near field light. The optical probe is a tapered optical fibre with 100 nm aluminium coat everywhere except at the tip. In this project along with these optical probes necessary electronics like PI feedback controller, high voltage amplifiers were made. For making optical probes, first a fibre pulling method is optimised and an aluminium coating process is optimised. A probe holder is designed and tuning fork with optical probe is attached on it. A separate piezo-tube assembly is made for the actuation of this probe. Few LabVIEW programs are written to automate this assembly and electronics. These programs are tested and optimised. Also an optical set-up is assembled to illuminate the sample with evanescent field.

There was some delay in getting FIB facility to prepare optical probe. But at the end we managed make those probes. Now the instrument works like an AFM and obtained some AFM images. The images shows that the motion control and LabVIEW programs are working as expected. The optical probe will be attached with PMT to finish the instrument.

# Contents

|          |  |           |
|----------|--|-----------|
| <b>1</b> | <b>Introduction</b>  | <b>3</b>  |
| 1.1      | The history . . . . .  | 3         |
| 1.2      | Our motivation . . . . .   | 4         |
| 1.3      | The instrument . . . . .   | 5         |
| <b>2</b> | <b>Theory</b>  | <b>6</b>  |
| 2.1      | Quantative force measurment from quartz-tuning fork. . . . .         | 6         |
| 2.2      | Electromagnetic wave on dielectric interface . . . . .               | 8         |
| 2.2.1    | Maxwell's equations . . . . .  | 8         |
| 2.2.2    | Total internal reflection and Evanescent waves . . . . .             | 8         |
| 2.3      | Frustrated total internal reflection or Optical tunnelling . . . . . | 11        |
| <b>3</b> | <b>Methods</b>   | <b>12</b> |
| 3.1      | Building the experimental set-up . . . . .                           | 14        |
| 3.1.1    | Optical fibre probe . . . . .  | 14        |
| 3.1.2    | XYZ Actuation . . . . .  | 18        |
| 3.1.3    | Probe assembly . . . . .   | 21        |
| 3.1.4    | Optical assembly . . . . .   | 21        |
| 3.1.5    | Electronics . . . . .  | 23        |
| 3.2      | LabVIEW Programs . . . . .   | 30        |
| 3.3      | Calibration of Scanner piezo . . . . .                               | 30        |
| <b>4</b> | <b>Results</b>   | <b>32</b> |
| <b>5</b> | <b>Discussion</b>  | <b>37</b> |
| 5.1      | The instrument as AFM . . . . .                                      | 37        |
| 5.2      | The instrument as NSOM . . . . .                                     | 38        |
| 5.3      | In Future . . . . .  | 38        |
|          | <b>References</b>  | <b>39</b> |

# Chapter 1

## Introduction

This chapter provides an introduction to the purpose and design of the instrument developed. Along with the motivation it will discuss some its unique features .

### 1.1 The history

We humans always find it easy to accept and believe things which we see in front our eyes rather than things we don't see. For instance, before telescopes people used to believe that earth as the centre of the universe and everything revolves around earth. And invention of microscope gave a tremendous boost in the development of science, especially in biology and material science. These inventions gave motivation to develop new technologies to see things with better resolution. In late 19th century, Abbe and Rayleigh showed there is a limitation in improving the resolution of normal optical microscopy. The minimum separation one can detect is around  $\lambda/2$ . Then efforts were made to push this limitation. In 1928 Synge [1] proposed the idea of a scanning near field optical microscope. According to his idea an image can be constructed by scanning a sample with a small aperture and recording the intensity of light through the aperture. And the resolution is limited by the aperture dimension. When the aperture is smaller than the wavelength of light used for illumination, then only a near field component will pass through the aperture. So we can call this kind of microscopes as "near-field scanning optical microscopes(NSOM). But precise actuation techniques were not yet available then. In 1956 O'Keefe proposed similar idea of Synge[2], but still the problem of actuation was unresolved. At the end of his paper O'Keefe mentions: "The realisation of this proposal is rather remote, because of the difficulty of providing for relative motion between the pinhole and the

object, when the object must be brought so close to the pinhole.". This concept of scanning with an aperture was first realised in 1972 by Ash and Nichols using microwaves( $\lambda = 10cm$ ) and obtained a resolution of  $\lambda/60$ [3]. In the same year,1972, Russell Young, John Ward and Fredric made a Microtopographer, a scanning probe profiler which used piezo electric actuators[4]. In 1982, scanning tunnelling microscope(STM)[5] was invented by Binning et al. which was the first scanning probe microscope to achieve atomic resolution. Now the precise actuation was available and NSOM was realised by Pohl et al. [6]and Lewis et al.[7] simultaneously in 1984. In the mean time, Atomic Force Microscope(AFM) was built by Binning et al. [8]. Later Betzig et al. further developed and applied NSOM[9, 10, 11] to study various things like optical spectroscopy of quantum wire structures. The NSOM offers an unique capability of optical access to zepto-liter volume, of the order of  $10^{-18}$  to  $10^{-20}$  liters. This provides an excellent opportunity to perform optical spectroscopy on such volumes.

## 1.2 Our motivation

Our instrument is built mainly for doing experiments on nano-confined water. Nano-confined water means the water between two flat surfaces which are separated by a few nano-meters, which is of the order of water molecule size.

Water, as we all know is the important factor for life in Earth. If you look at the basic building blocks of life, the cells, it's main constituent is water. Most of the cell processes and molecular machines (eg: intermembrane-ion-channels) in cells works in nano-volumes of water. In-order to study these molecular machines, first we should have a clear physical picture, how nano-volumes of water behaves? Will it behave like bulk water? Is the viscosity of nano-volumes of water different from bulk water? These are some of the interesting questions people are currently working on. People use Surface Force Apparatus(SFA)[12, 13, 14] or AFM[15, 16] to study nano-volumes of water. Unfortunately, we still don't have a clear understanding of nanoconfined water[17]. AFM studies on confined water indicates a viscoelastic behaviour[16] while studies done on SFA shows confined water to have same behaviour as bulk water[14]. But SFA studies on non-polar liquids like OMCTS(Octamethylcyclotetrasiloxane) did show viscoelastic behaviour[12, 13]. In order to explain these behaviours we should have a clear molecular picture of these confined liquids.

One way to understand the molecular picture of confined liquids is to measure diffusion coefficient of some fluorescent dye moving through the confined



liquid. A shear force AFM can be used to measure mechanical properties of water [18, 16]. Along with that if we can pass light through the confined liquids and measure the intensity fluctuations as a dye move through the confined liquid, we can measure diffusion coefficient. A NSOM with shear force measurement capability can do such a measurement.

One interesting conjecture[16] proposed by our labouratory from the current mechanical measurements is that on confinement water spontaneously arrange themselves in confined volume like solid and this transition is like a phase transition. If it is like second order phase transition then on confinement it should show a critical opalescence, which could be detected with an NSOM.

### 1.3 The instrument

The reports of AFM with quartz tuning fork as the force sensor exist in literature. Such an AFM achieved atomic resolution[19]. Most of the NSOM available today use quartz tuning fork as a force sensor and use it only in feedback mechanism to keep the NSOM tip at a constant separation from sample. The prime difficulty with quartz tuning fork is, being a non-linear oscillator, quantification of force from its signal is not a trivial task. Recently there are some theoretical models which allow to do quantitative force measurements with tuning forks[20, 18] for q-plus arrangement of tuning fork[21].(Details of this theory is given in chapter 2).Our instrument will be the first one which incorporates this theory in an NSOM, along with optical measurements for molecular mobility

Using this instrument we will be able to do force measurement along with near-field detection. That is the unique feature of this instrument.

# Chapter 2

## Theory

This chapter describes the basic theory which helps us to understand the working of the instrument and data interpretation. The chapter first discusses a theoretical model for quantitative estimation of forces from a quartz-tuning fork based force sensor. Then a basic introduction to evanescent field is given. The chapter ends with a discussion of the phenomenon on which the nearfield optical microscopes are based, which is called frustrated total internal reflection.

### 2.1 Quantative force measurment from quartz-tuning fork.

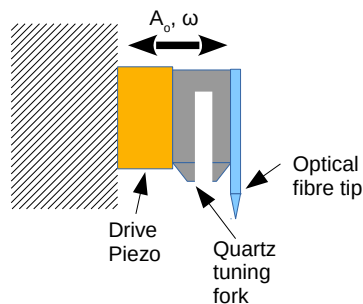


Figure 2.1: **Q-plus arrangement**[21] . Quartz tuning fork as force sensor in q-plus arrangement.

The instrument uses quartz tuning fork in q-plus[21] arrangement as the force sensor which gives a current output proportional to the differential bending between the prongs of the tuning fork. The q-plus arrangement with mechanical drive is given in figure 2.1.

In this arrangement one prong of the tuning fork is attached to the drive piezo which is attached to a stationary base and the other prong is free to oscillate with the tip. The tip is allowed to interact with the sample. Using the drive piezo, the tuning fork is oscillated in a frequency  $\omega$  and amplitude  $A$ . If  $k$  is the equivalent spring constant of the tuning fork,  $b$  is the damping coefficient and  $x$  is the displacement of the tip, then equation of motion for the tip can be written as:

$$m\ddot{x} + b\dot{x} + kx = F \cos(\omega t) + F_{int} \quad (2.1)$$

$x(t) = A \sin(\omega t + \theta)$  is a solution for this equation. Equation 2.1 can be rearranged as :

$$\begin{aligned} F_{int} &= m\ddot{x} + b\dot{x} + kx - F \cos(\omega t) \\ &= m\ddot{x} + b\dot{x} + kx - F \cos(\omega t + \theta - \theta) \\ &= m\ddot{x} + b\dot{x} + kx - F \sin(\omega t + \theta) \sin(\theta) - F \cos(\omega t + \theta) \cos(\theta) \\ &= m\ddot{x} + b\dot{x} + kx - \frac{F}{A} A \sin(\omega t + \theta) \sin(\theta) - \frac{F}{A\omega} A\omega \cos(\omega t + \theta) \cos(\theta) \\ &= m\ddot{x} + b\dot{x} + kx - \frac{F}{A} x \sin(\theta) - \frac{F}{A\omega} \dot{x} \cos(\theta) \text{ here } \ddot{x} = \omega^2 x \\ &= (m\omega^2 + k - \frac{F}{A} \sin(\theta))x + (b - \frac{F}{A\omega} \cos(\theta))\dot{x} \\ &= -k_{int}x - b_{int}\dot{x} \end{aligned} \quad (2.2)$$

$$\text{where, } k_{int} = -m\omega^2 - k + \frac{F}{A} \sin(\theta) \quad (2.3)$$

$$b_{int} = -b + \frac{F}{A\omega} \cos(\theta) \quad (2.4)$$

Where,  $m, b$  and  $F$  can be calculated from the experimental parameters [20].

$$m = \frac{k}{\omega_0^2} \text{ here, } \omega_0 \text{ is the resonance frequency of the tuning fork.} \quad (2.5)$$

$$b = \frac{k}{Q\omega_0} \text{ here, } Q \text{ is the quality factor of the tuning fork.} \quad (2.6)$$

$$F = \frac{kA_0}{Q} \text{ here, } A_0 \text{ is the resonance amplitude.} \quad (2.7)$$

Thus from the experiment we will be able to calculate  $k_{int}$  and  $b_{int}$  which tell us the contribution of elastic and dissipative forces in the interaction force.

## 2.2 Electromagnetic wave on dielectric interface

Behaviour of Electromagnetic waves(EM waves) on the interface between two dielectric can be explained using Maxwell's equations and its boundary conditions.

### 2.2.1 Maxwell's equations

Maxwell's equation on a dielectric medium without any embedded charges or current can be written as:

$$\left. \begin{aligned} \nabla \cdot \mathbf{D} &= 0 \\ \nabla \times \mathbf{E} &= -\frac{\partial \mathbf{B}}{\partial t} \\ \nabla \cdot \mathbf{B} &= 0 \\ \nabla \times \mathbf{H} &= \frac{\partial \mathbf{D}}{\partial t} \end{aligned} \right\} \quad (2.8)$$

Where, for a linear medium

$$\begin{aligned} \mathbf{D} &= \epsilon \mathbf{E} \\ \mathbf{H} &= \frac{1}{\mu} \mathbf{B} \end{aligned}$$

### 2.2.2 Total internal reflection and Evanescent waves

When an electromagnetic wave encounter a discontinuity in dielectric medium, at the interface of the discontinuity, the wave is split into a transmitted and a reflected wave. The angle of the transmitted wave  $\theta_t$  with respect to normal of the interface is given by Snell's law. Here, interface is between medium 1 and 2 and they have  $n_1 = \sqrt{\epsilon_1 \mu_1}$  and  $n_2 = \sqrt{\epsilon_2 \mu_2}$  as there refractive indices. and  $\theta_i$  is the angle of incidence.

$$\frac{\sin(\theta_i)}{\sin(\theta_t)} = \frac{n_2}{n_1} \quad (2.9)$$

With respect to incident plane (the plane which contain incident ray and normal), we can resolve the electric field into two polarisations one perpendicular ( $E^\perp$ ) to incident plane and another parallel ( $E^\parallel$ ) to incident plane as well as perpendicular to propagation vector ( $\mathbf{k}$ ). Any polarisation can be decomposed to these two polarisations.

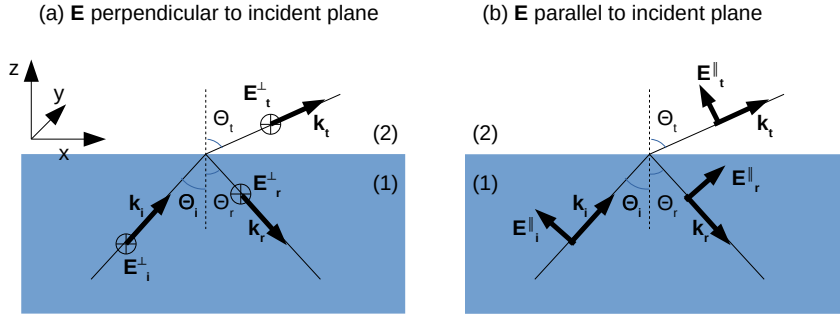


Figure 2.2: **Interface between dielectric media.** Electromagnetic wave travelling through an interface between two dielectric media

The amplitudes of the transmitted and reflected waves are given by the Fresnel coefficients. Let  $\mathbf{E}_i, \mathbf{E}_r$  and  $\mathbf{E}_t$  respectively be the incident, reflected and transmitted amplitudes. Then for both polarisations we can write:

$$E_r^\perp = E_i^\perp \times \mathcal{R}^\perp \quad (2.10)$$

$$E_t^\perp = E_i^\perp \times \mathcal{T}^\perp \quad (2.11)$$

$$E_r^\parallel = E_i^\parallel \times \mathcal{R}^\parallel \quad (2.12)$$

$$E_t^\parallel = E_i^\parallel \times \mathcal{T}^\parallel \quad (2.13)$$

where  $\mathcal{R}^\perp, \mathcal{T}^\perp, \mathcal{R}^\parallel$  and  $\mathcal{T}^\parallel$  are the Fresnel coefficients. They are given

by[22]:

$$\mathcal{R}^\perp = \frac{\cos \theta_i - n_r \cos \theta_r}{\cos \theta_i + n_r \cos \theta_r} \text{ where } n_r = \frac{n_2}{n_1} \quad (2.14)$$

$$\mathcal{T}^\perp = \frac{2 \cos \theta_i}{\cos \theta_i + n_r \cos \theta_r} \quad (2.15)$$

$$\mathcal{R}^\parallel = \frac{\cos \theta_r - n_r \cos \theta_i}{\cos \theta_r + n_r \cos \theta_i} \quad (2.16)$$

$$\mathcal{T}^\parallel = \frac{2 \cos \theta_r}{\cos \theta_r + n_r \cos \theta_i} \quad (2.17)$$

The electric field in medium 2 can be written in x,y and z co-ordinates as :

$$\mathbf{E}_2 = \begin{bmatrix} -E_1^\parallel \mathcal{T}^\parallel \sin \theta_t \\ E_1^\perp \mathcal{T}^\perp \\ E_1^\parallel \mathcal{T}^\parallel \cos \theta_t \end{bmatrix} e^{-i(\mathbf{k}_2 \cdot \mathbf{r} - \omega t)} \quad (2.18)$$

Since due to boundary conditions  $k_x$  and  $k_y$  will not change in medium 1 and 2. So we can write:

$$\begin{aligned} k_{z2} &= \sqrt{k_2^2 - (k_x^2 + k_y^2)} \text{ but } \sqrt{k_x^2 + k_y^2} = k_1 \sin \theta_i \\ &= \sqrt{k_2^2 - k_1^2 \sin^2 \theta_i} \\ &= k_2 \sqrt{1 - \left(\frac{k_1}{k_2}\right)^2 \sin^2 \theta_i} \text{ but } k = \frac{\omega}{v} \text{ so } \frac{k_1}{k_2} = \frac{v_2}{v_1} = \frac{n_1}{n_2} \\ &= k_2 \sqrt{1 - \left(\frac{n_1}{n_2}\right)^2 \sin^2 \theta_i} \end{aligned} \quad (2.19)$$

Now assume  $n_1 > n_2$  then  $\frac{n_1}{n_2}$  is a quantity greater than one. At a certain angle of incidence  $\theta_i = \theta_c$  the transmission angle  $\theta_t = \frac{\pi}{2}$ . This angle of incidence is called **critical angle**. At critical angle we have:

$$\sqrt{1 - \left(\frac{n_1}{n_2}\right)^2 \sin^2 \theta_c} = 0 \text{ since } \frac{n_1}{n_2} = \frac{1}{\sin \theta_c} \text{ from snell's law} \quad (2.20)$$

So above critical angle  $k_{z2}$  (equation 2.20) is complex. The equation 2.18 can be rewritten as:

$$\mathbf{E}_2 = \begin{bmatrix} -E_1^\parallel \mathcal{T}^\parallel \sin \theta_t \\ E_1^\perp \mathcal{T}^\perp \\ E_1^\parallel \mathcal{T}^\parallel \cos \theta_t \end{bmatrix} e^{-i(xk_x + yk_y - \omega t)} e^{-\gamma z} \text{ where } \gamma = k_2 \sqrt{\left(\frac{n_1}{n_2}\right)^2 \sin^2 \theta_c - 1} \quad (2.21)$$

This equation tells that, the wave propagate only along the interface not along  $z$ . Along  $z$  the wave is not propagating and it is just oscillation in time and dies off exponentially along  $z$ . This exponentially decaying wave is called **evanescent wave or near field**. When angle of incidence is critical angle or above critical angle an evanescent field is created in medium 2 and most of the wave is reflected back in medium 1. This is called **total internal reflection**.

## 2.3 Frustrated total internal reflection or Optical tunnelling

Frustrated total internal reflection is considered to be an optical analog of quantum mechanical tunnelling effect[22]. Consider a third medium above the medium 2 in the previous system of two media such that  $n_1 > n_3 > n_2$ . And  $\theta_i > \theta_c$ , thus an evanescent field is created in medium 2. When the medium 3 is sufficiently close to interface of medium 1 and 2. Then evanescent field interact with medium 3 and a far-field light is propagated through the medium 3[23]. This phenomenon is called **frustrated total internal reflection or optical tunnelling**. This concept is utilised in super-resolution microscope called Near-field Scanning Optical Microscope(NSOM).

Thus we can measure forces form the tunning fork with tip and can use same optical fibre tip to collect near field light through frustrated total internal reflection. That's the basic theory for the instrument.

# Chapter 3

## Methods

The experimental set-up is a combination of atomic force microscope (AFM) and a near-field scanning optical microscope (NSOM). Here AFM senses lateral shear forces using a quartz tuning fork. And NSOM works by far-field illumination and near-field detection. The sample is illuminated by near-field light and a far-field light is detected from small glass optical aperture which can scan over the sample. Basic schematic of the experimental set-up is shown in the figure 3.1.

Here we have a piezo electric quartz tuning fork with its one leg attached to a drive piezo and the other leg to an aluminium-coated, tapered optical fibre (Q-plus arrangement [21]). Using the drive piezo, tuning fork is oscillated at its resonance frequency. The oscillations produce differential bending between the legs of tuning fork. Thus a strain is developed in tuning fork prongs. As the tuning fork is piezoelectric, strain leads to generation of current. This current is of the order of nano-amperes, so we have to use a pre-amplifier with a large gain ( $10^7 I/V$ ). The magnitude of this current decreases when the attached fibre-tip is brought sufficiently close to the glass surface with sample. This reduction in the current is due to the tip-sample-surface interaction acting as the drag force for the oscillation of tuning fork. Thus the current from tuning fork is a measure of the tip's interaction forces. The root-mean-square value of current amplitude along with its phase with respect to drive is measured using a lock-in amplifier. By using a suitable conversion method described in chapter 2, one can relate measured amplitude and phase to shear force experienced by the tip. This is how we can sense forces. By driving the tuning fork at very low off-resonance frequency we can even quantify the sensed force and can calculate the viscosity of the sample [18, 16].



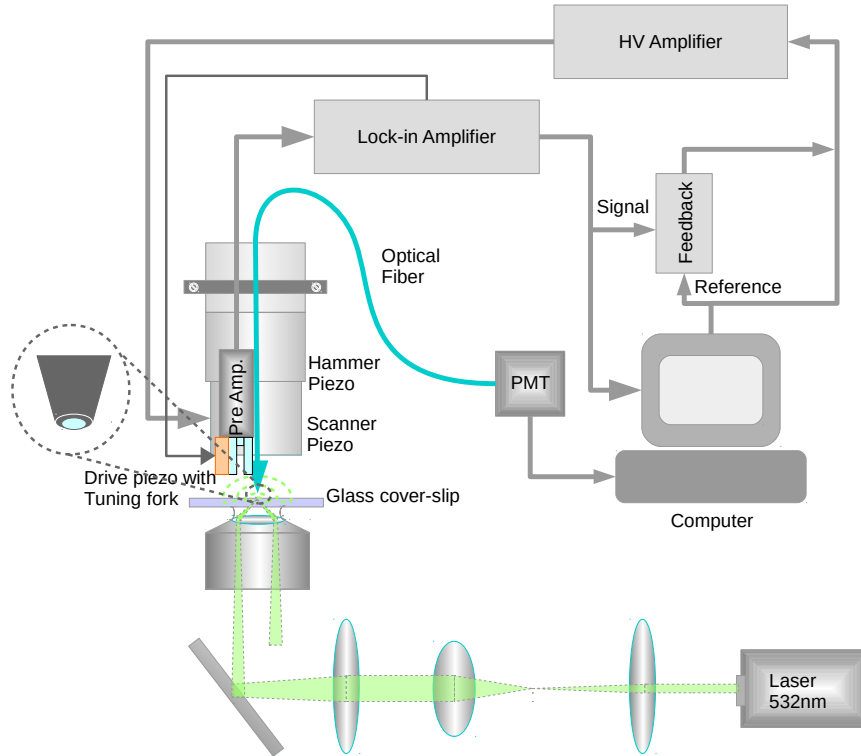


Figure 3.1: **Basic schematic of the set-up.** This is the basic schematic of the experimental set-up

The fibre tip have 100nm thick aluminium coating everywhere except at the extreme end of the tip, thus we have an aperture at the tip. Depending on the sharpness of the fibre tip, the aperture size varies and typical aperture diameter is around 100nm. This aperture is positioned over the sample taken over glass cover slip. Below the cover-slip an oil immersion-objective with high numerical aperture(1.6 N.A.) is kept. And an optical arrangement is done such that total internal reflection happens at glass-sample interface. This total internal reflection makes a non-propagating evanescent light on the side of the optical fibre tip. And this evanescent wave interact with sample and aperture at the tip and results a frustrated total internal reflection/optical tunnelling. Due to this, far-field light is obtained at the other end of the fibre and is collected using a Photo-Multiplier Tube(PMT). This is our optical signal

## 3.1 Building the experimental set-up

### 3.1.1 Optical fibre probe

Optical fibre probe is a tapered optical fibre with aluminium coating everywhere except at the extreme tip.

#### Step1: Making a tip out of optical fibre

Fibre tips are made using micro-pipette puller(Shutter P2000). The bare optical fibre(Thor labs 460HP) used has  $125\mu m$  in diameter. In order to make a tip, the fibre is loaded on a micro-pipette puller and fixed under a tension. Then a  $CO_2$  laser is focused on the fibre and it start melting. Since the fibre is under a tension, when melting happens, fibre elongates and forms an elongated hourglass structure at the focus. As it elongates, it will cross a prescribed velocity. Then the laser is turned off and a hard pull is initiated. Due to this hard pull, fibre breaks and a tapered region is formed at the broken end. This is our fibre tip. A basic schematic of the set-up is given in figure 3.2

The parameters to set in the pulling instrument are the following:

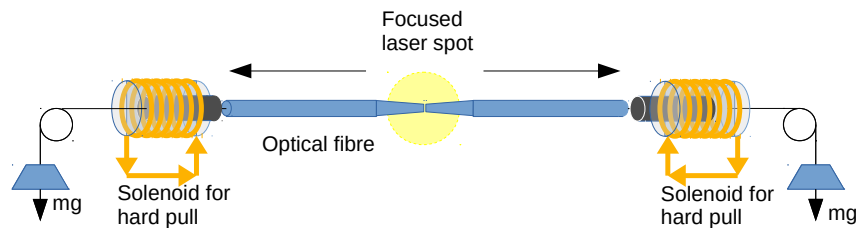


Figure 3.2: **Fibre Puller**. This is the schematic of the fibre puller

#### 1. Heat

This parameter sets the power of the laser. We can set the power in a scale of 0 to 999, such that 999 set the maximum power of the laser, that is 20W.

#### 2. Filament

By setting this parameter to some value between 0 to 15 sets the scan

length of the laser spot or the effective length to be exposed by the laser. In this scale 0 means 1mm.

### 3. Velocity

This is the set-point velocity to be reached to initiate the hard pull. Values are given from a scale of 0 to 255. The values are proportional to the millivolts generated in the transducer detecting velocity.

### 4. Pull

This sets the force for the hard pull. The parameter determine how much current to be provided for the solenoid to do the hard pull. The permissible current range is scaled to integers from 0 to 255.

### 5. Delay

This indicates in milliseconds when to turn off laser. Values can range from 0 to 255. And time is measured with respect to hard-pull initiation and that instant is offsetted with value  $128ms$ . So if we want to turn off laser  $xms$  before the hard pull, then the parameter will be  $128 - x$  and if it is  $xms$  after hard pull then  $128 + x$ .

These parameters are optimised to give tips with tip diameter approximately 50 to 60 nm. The optimized parameters are given in table 3.1

| Heat | Filament | Velocity | Delay | Pull |
|------|----------|----------|-------|------|
| 350  | 0        | 18       | 126   | 150  |

Table 3.1: Optimized parameters for fibre puller

An FSEM image of typical fibre without any coating is shown in figure 3.4

### Step2: Coating the fibre tip with aluminium

The fibre tip is coated with aluminium using a RF-Sputter coating set-up 3.3. While coating, fibre is kept perpendicular to the aluminium beam and is rotated along the fibre axis. A schematic drawing of the set-up is given in figure 3.3. Since the coating set-up doesn't has any thickness monitoring system, parameters of coating system is optimized to give 100 to 150 nm coat over fibre.

### Optimisation of coating system

Main parameters to optimise are RF power, argon pressure and coating time. This is done by coating a thin long glass cover slip at the place of fibre. After coating the coating thickness is masured using an AFM. Coating thickness is

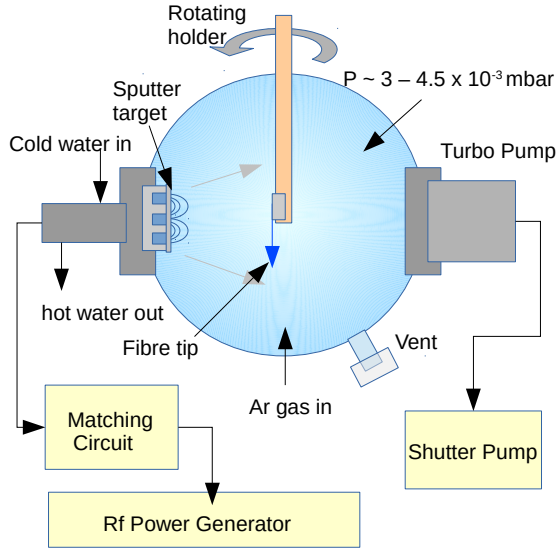


Figure 3.3: **RF-Sputter coating set-up.** This is a schematic drawing of the RF-Sputter coating set-up

obtained from the step height of the coated region with respect to uncoated region. And uncoated region is obtained by masking some area of the cover slip with scotch tape before coating and removing it after coating. The optimised parameters of the coating set-up to give 100 to 150nm is given in table 3.2.

|                 |  |
|-----------------|--|
| Rf Power        | 80W                                    |
| Pressure        | 3 to $4.5 \times 10^{-3} \text{ mbar}$ |
| Time of coating | 60 min                                 |

Table 3.2: Optimized parameters for RF-coating set-up

A typical coated fibre tip is shown in figure 3.5.

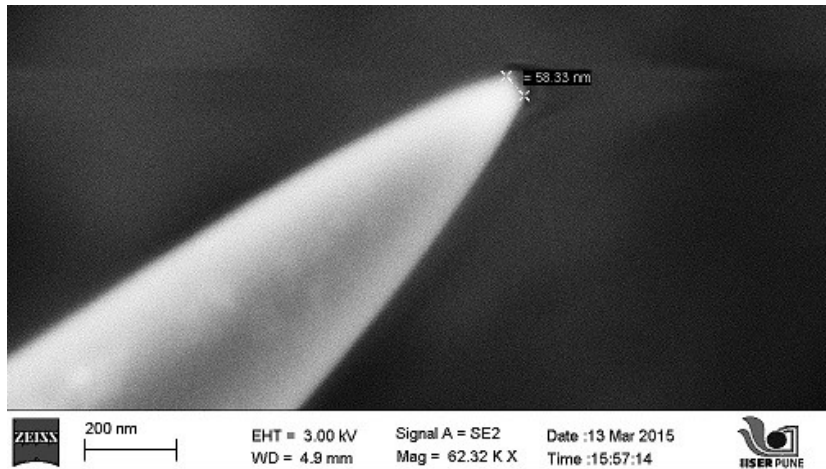


Figure 3.4: **Bare fibre tip.** This is a FSEM image of typical fibre without any coating and have tip diameter 58.33nm.

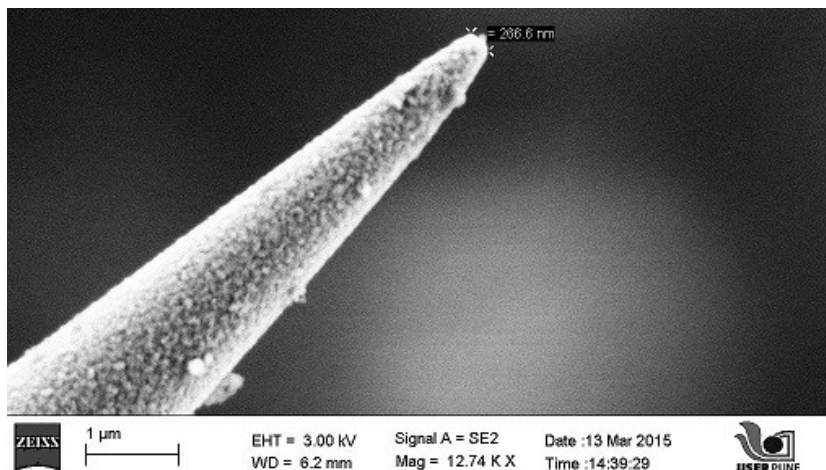


Figure 3.5: **Aluminium coated fibre tip.** This is a FSEM image of an aluminium coated fibretip. After coating tip diameter is 260 to 350nm.

### Step3: Obtaining an optical aperture at the tip

The required optical fibre probe should not have coating at the extreme tip. The coating at the extreme tip can be removed from a fully coated fibre by the use of Focused Ion Beam(FIB) microscope[24]. Using a focused ion beam one can slice out the coating from the end of the tip. This slicing is done by placing the coated fibre tip perpendicular to gallium ion beam(30kV, 0.10nA). After slicing a glass aperture with 200 to 300 nm diameter is exposed at the tip end. A coated fibre after slicing is shown in figure.

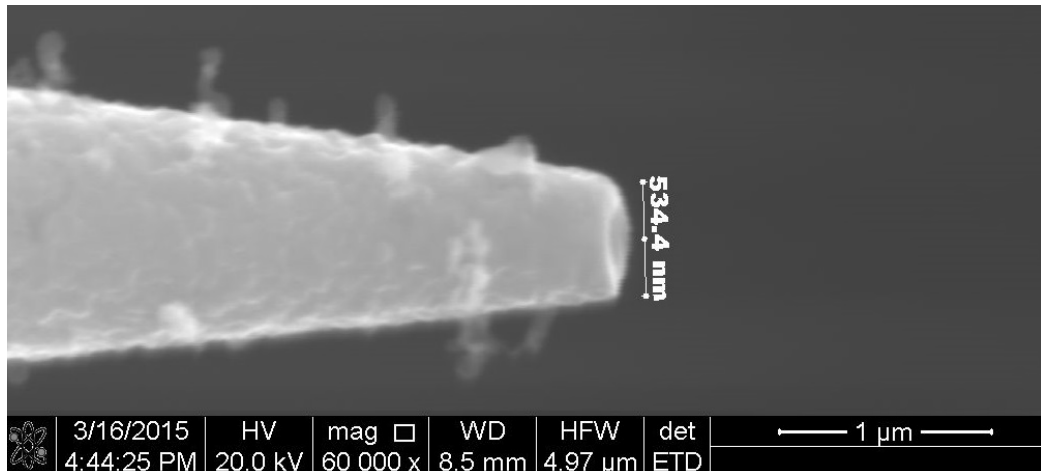


Figure 3.6: **FIB sliced-Aluminium coated fibre tip.** This is a FSEM image of an aluminium coated fibre tip after slicing the tip end with FIB.

### 3.1.2 XYZ Actuation

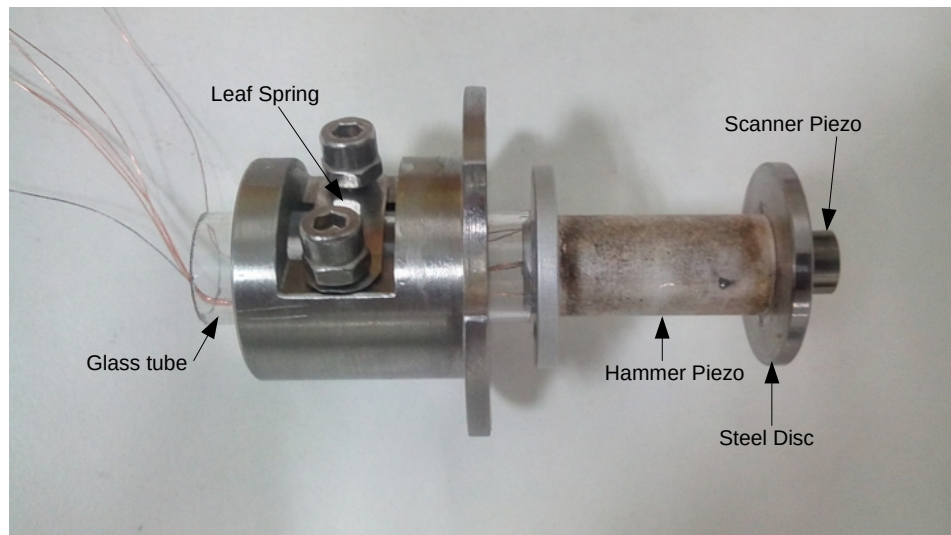


Figure 3.7: **Piezo tube assembly for XYZ motion.** This is the piezo tube assembly which is used for the x,y and z motion of the probe

The X,Y and Z motion is achieved using piezo electric tubes[18, 25]. Coarse Z movement is achieved using a hammer piezo and fine movement in X,Y and Z is done using a scanner piezo. An actual piezo assembly for these motion is shown in figure 3.7.

### Coarse movement in Z: Inertial Sliding Mechanism

Coarse movement in Z is achieved using hammer piezo. And inertial sliding is the mechanism with which it works.

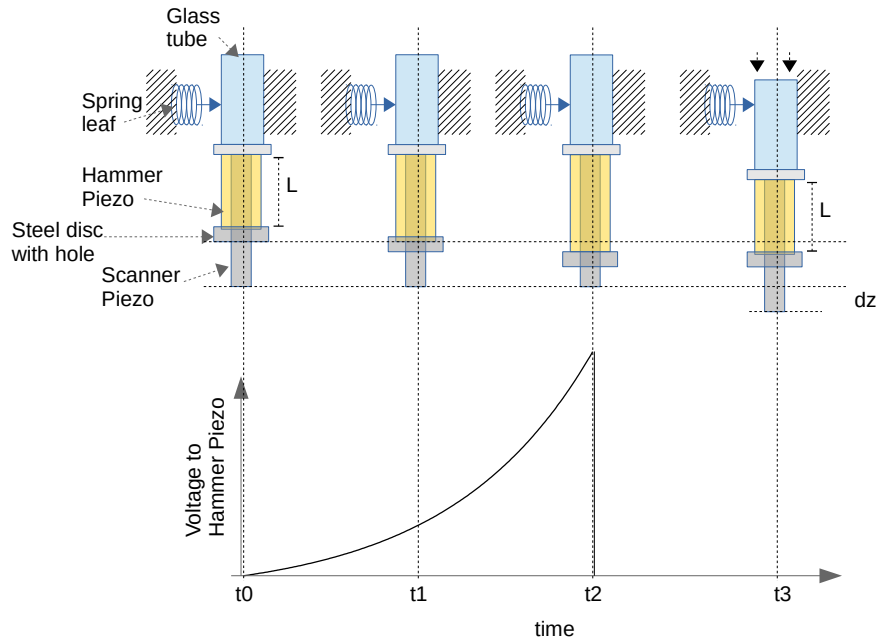


Figure 3.8: **Coarse motion in Z.** Coarse motion in Z is done using inertial sliding mechanism

The figure 3.8 illustrates how coarse movement in z is achieved using inertial sliding mechanism. In the piezo assembly (figure 3.7) one end of the hammer piezo tube is attached to a steel disc and another to an aluminium disc. And to the other side of this aluminium disc a glass tube is attached. Whole assembly is held in place by a leaf spring, pressing over this glass tube. As shown in figure 3.8, as we slowly increase voltage applied to hammer piezo, the hammer piezo elongates, keeping the glass tube in same position. But

when the voltage suddenly drops, hammer piezo regains its original length. While it contracts back its original length, as the steel plate attached to one end of hammer piezo have more inertia than the other end, it pulls down the glass tube. Thus whole assembly slides down a small step  $dz$  along  $z$ . If we apply an opposite pulse to the hammer piezo, then the whole assembly moves in the opposite direction.

### **X,Y, Z fine motion**

Fine motion in  $x$ ,  $y$  and  $z$  is done using a scanner piezo. The scanner piezo have one common ground connected to inner surface of the tube and four symmetric electrodes along the outer surface.(figure 3.9)

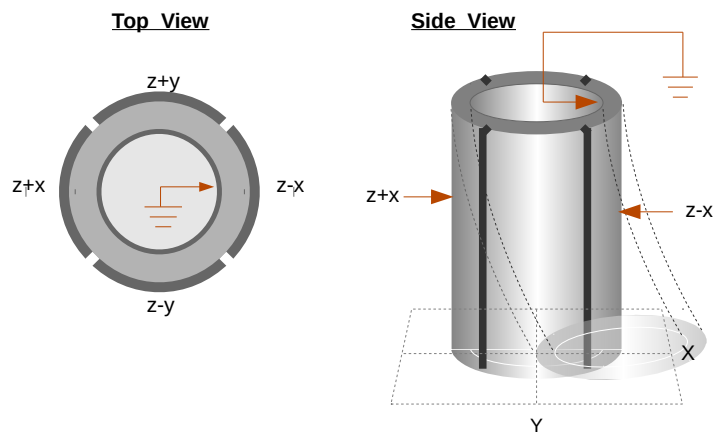


Figure 3.9: **Scanner tube piezo.**

Fine motion in  $z$  is achieved by giving a  $z$  voltage to all four electrodes on outside surface of scanner piezo. Depending in the sign of the  $z$  voltage, the scanner tube either elongated or contracts.

For  $x$ ,  $y$  motion along with the  $z$  voltage, specific voltages are given to individual electrodes on the outer surface. Electrodes along  $x$  and  $y$  direction gets equal and opposite voltages along with  $z$  voltage. So for electrodes along  $x$  will receive  $z+x$  and  $z-x$  voltages and along  $y$  it is  $z+y$  and  $z-y$ .

For movement along  $x$  axis, when electrodes along  $x$  axis receives  $z+x$  and  $z-x$  voltages, the side which receives more voltage than the other will elongate and the other side will shorten. Thus it result a slight bending in scanner



tube and one end of the tube is displaced along x with respect to the other end. This bending will not give rise to any detectable angle. Because the bending here gives only a few  $\mu m$  displacements and length of the tube is 3cm.

Similarly we get y motion and combination of x,y and z motion.

### 3.1.3 Probe assembly

In-order to fix the tuning fork assembly to the scanner piezo a probe holder base and a probe holder has been designed. Tuning fork along with drive piezo and fibre tip is fixed on the probe holder (figure 3.10).

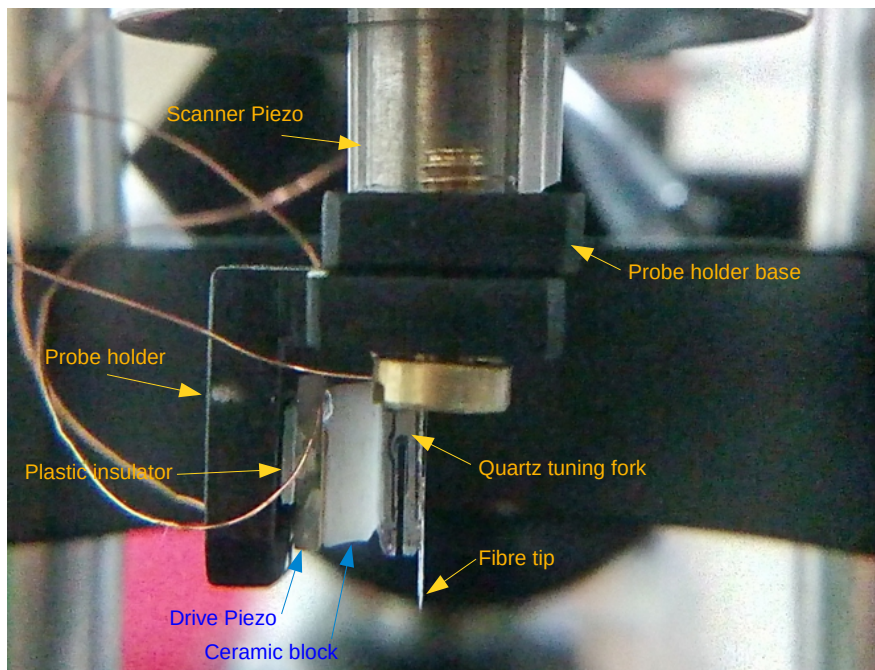


Figure 3.10: **Probe assembly**. This figure shows how tuning fork with drive piezo and fibre tip is attached to scanner piezo

### 3.1.4 Optical assembly

The ray diagram of the optical set-up is given in figure 3.11.

The main aim of the optical set-up is to get total internal reflection at the interface of cover slip and sample/water, collect the near-field light created and detect it with PMT. The main components in the optical set-up are :

- Laser source (coherent, 532nm)
- Beam expander (telescopic arrangement)
- Converging lens (convex lens,  $f=300\text{mm}$ )
- High N.A objective (Olympus, Oil immersion, 60x, N.A =1.6)
- Near-field optical probe
- PMT (HAMAMATSU H9307-02)

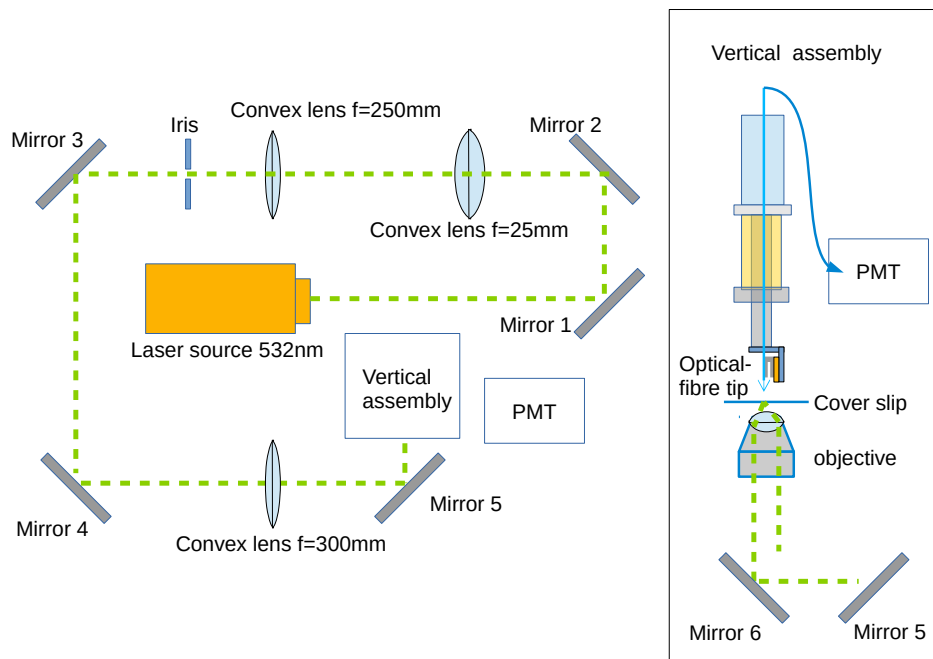


Figure 3.11: Ray diagram for optical set-up.

With the help of mirrors all these components are compactly arranged on an optical bread-board. These are aligned to get total internal reflection at the interface of cover slip and sample/water. Such an arrangement without PMT and optical probe is shown in figure 3.12

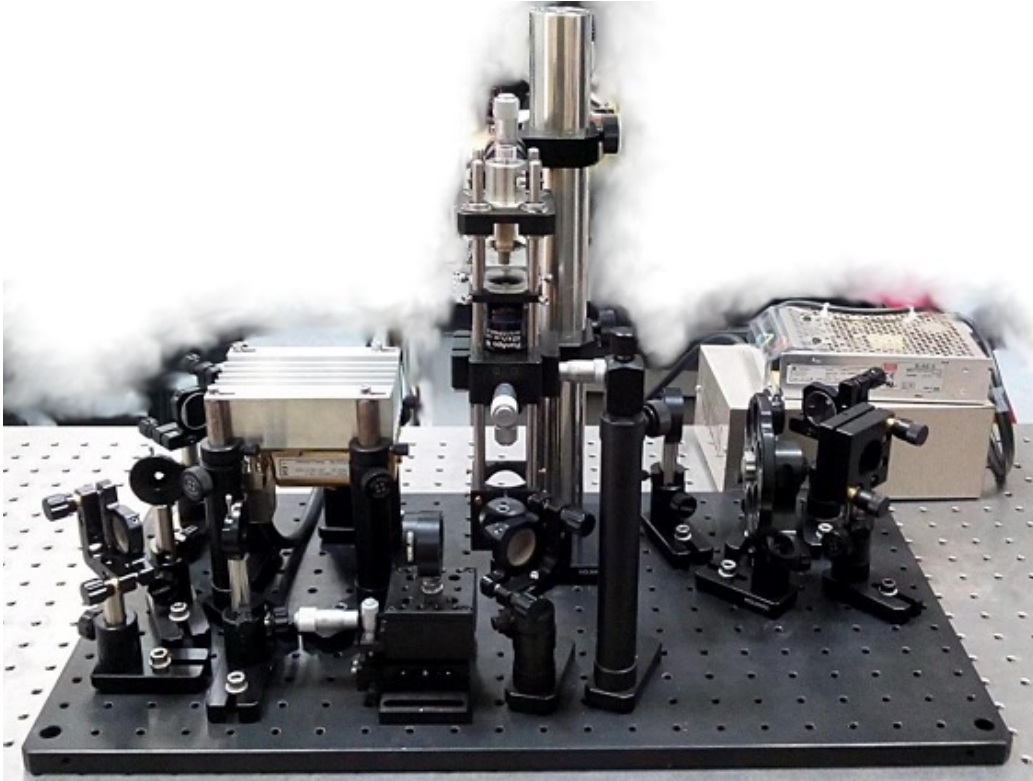


Figure 3.12: **Optical set-up without PMT.**

### 3.1.5 Electronics

The schematics of the basic electronics set-up is shown in figure 3.13

Pre-amplifier signal from tuning-fork will vary with  $z$ -position of fibre tip, provided fibre tip is sufficiently close to glass slide. Since the tuning-fork is oscillated with a drive piezo, the signal from tuning fork is amplitude modulated. And signal is demodulated using AD630 IC. This signal is given to PI Controller to compare with a reference voltage and provide a voltage output to scanner piezo so that, signal and reference match. Using the relay-1 we can switch the source of  $z$ -voltage between computer and PI Controller. But this switching from PI controller to computer or vice versa will give a momentarily zero voltage a  $z$ -voltage. This is avoided by the use of a capacitor. This capacitor will be charged to the same  $z$ -voltage before switching and it will provide this voltage at the time of switching. Connection of capacitor is controlled by relay 2, and it is connected only for small interval which over-

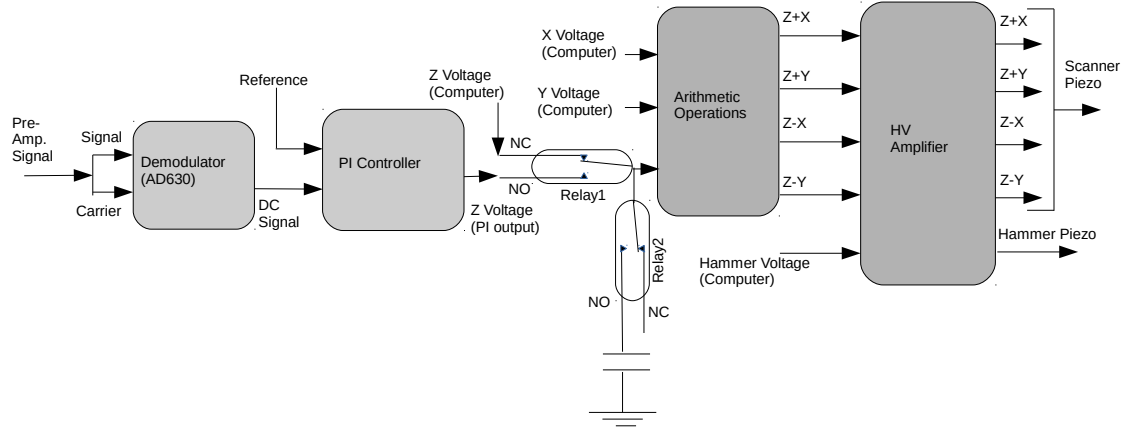


Figure 3.13: **Schematics of basic electronics set-up.** This is the schematics of basic electronics set-up required

lap the switching process. This z-voltage along with x and y voltages from computer are given to electronic circuits to perform arithmetic operations and obtain four different voltages  $z+x$ ,  $z-x$ ,  $z+y$  and  $z-y$ , since scanner piezo require these voltages. These voltages are amplified using High Voltage(HV) Amplifiers and feed to scanner piezo.

### 1. Demodulator

Demodulator is made using AD630 IC as per the circuit diagram given in data sheet for AD630 from 'Analog Devices'. Same circuit diagram is reproduced as figure 3.14.

Demodulator circuit is tested with 30Khz sine wave. This frequency is chosen because, the signal from tuning fork will have a similar frequency. Here in the testing modulation input and carrier input are the same sine wave. This circuit converts an AC signal to some DC amplitude which is proportional to the peak to peak voltage of the signal.

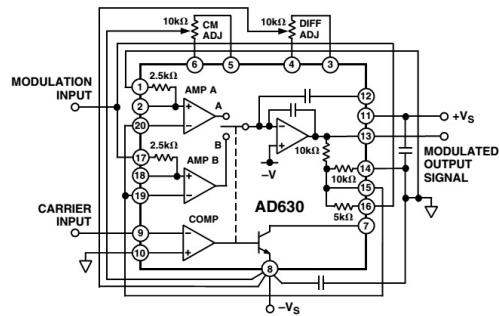


Figure 3.14: **Circuit diagram of demodulator.** This is the circuit diagram for demodulator (image source: data sheet of AD630 from Analog Devices)

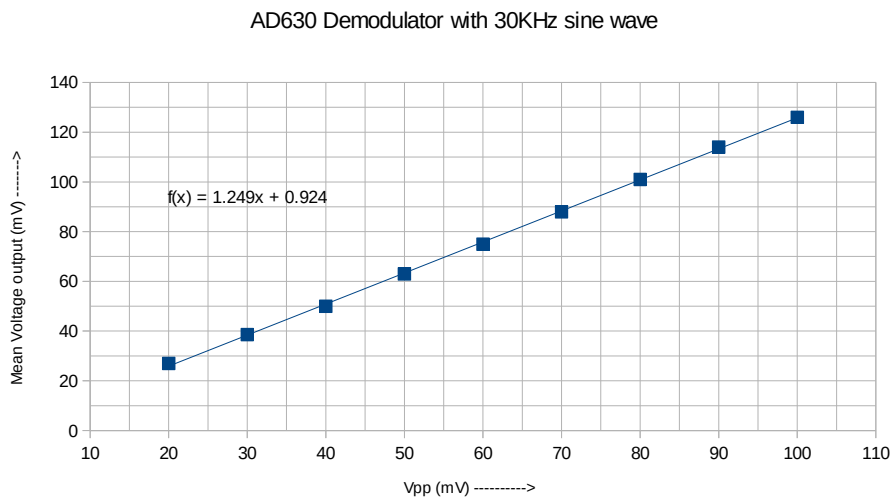


Figure 3.15: **Testing demodulator.** This is the demodulator output when same 30KHz sine wave is given as modulation and carrier inputs

## 2. PI controller

PI controller is made as per the circuit given in figure 3.16

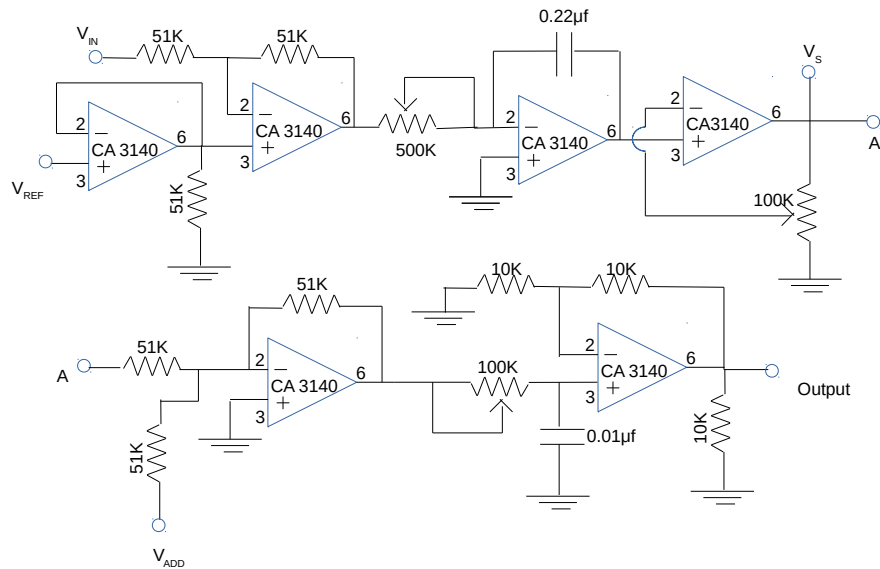


Figure 3.16: **Circuit for PI controller.**

PI controller is checked and found that it is actively controlling the z position of fibre tip to give a prescribed signal amplitude from tuning fork.

### 3. Electronics for Arithmetic operations

From the x, y and z voltages from computer we need to calculate  $z+x$ ,  $z+y$ ,  $z-x$  and  $z-y$  voltages. So we need two addition and two subtraction circuits. Circuits which do addition and subtraction of voltages are given in figure 3.17

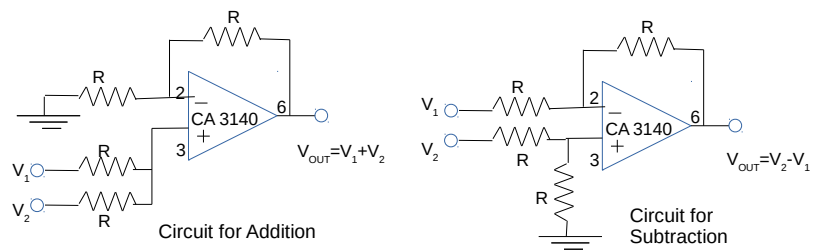


Figure 3.17: **Circuit for addition and subtraction.**

#### 4. High voltage amplifiers

High voltage amplifiers are made using PA88 op-amps. Circuit diagram of an amplifier is given in figure 3.18.

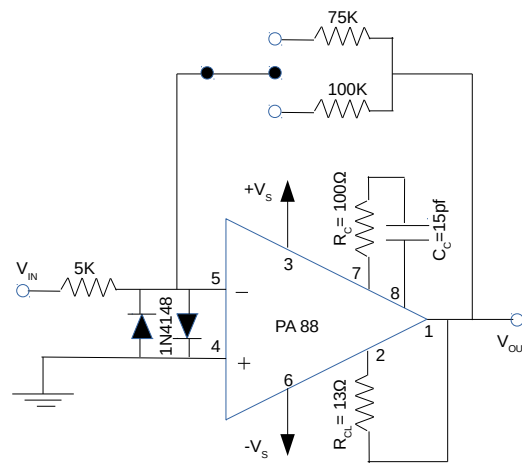


Figure 3.18: **Circuit for high voltage amplifier.** Circuit which uses PA88 IC for high voltage amplification

The IC PA88 is driven using a 225V dual DC voltage supply(Ultra Volt 1/4C24). Six of such amplifiers are made; One to drive hammer piezo, four to drive scanner piezo and one extra. Each amplifier have switch-able gains of 15 and 20. For these gains, typical DC amplification response is plotted and shown as figure 3.19.

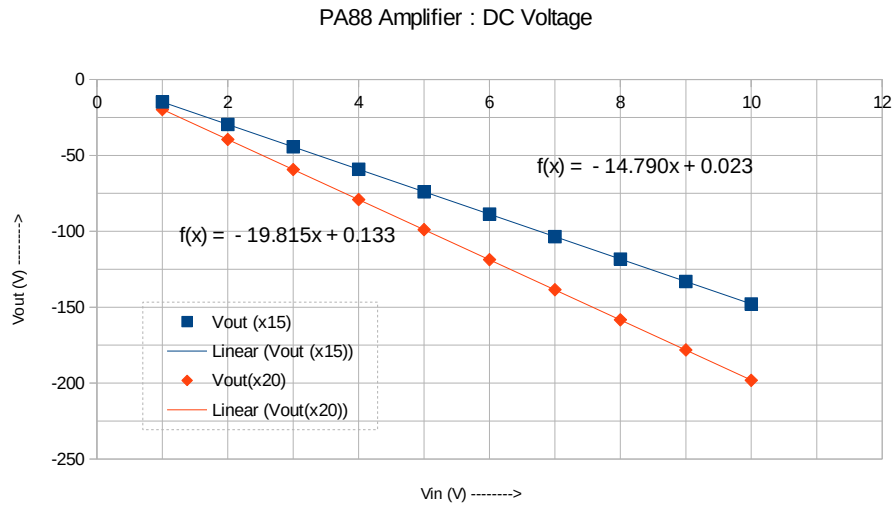


Figure 3.19: **Testing high voltage amplifier.** DC amplification is tested by giving DC input voltage and recording the output voltage from the amplifier

The amplifier works as an inverting amplifier and it have switch-able gains of 19.8 and 14.8.

### Assembling all the circuits in a box

All the circuits are made and assembled them in a box.





Figure 3.20: **Controller Box**. All the electronics are arranged in an instrument box (a)the front panel (b)the back panel (c) inside the box:top view

## 3.2 LabVIEW Programs

The experimental set-up is controlled using programs written in LabVIEW language via a data acquisition card( NI USB6363).

The front panel of the main program for data acquisition is given in figure 3.21.

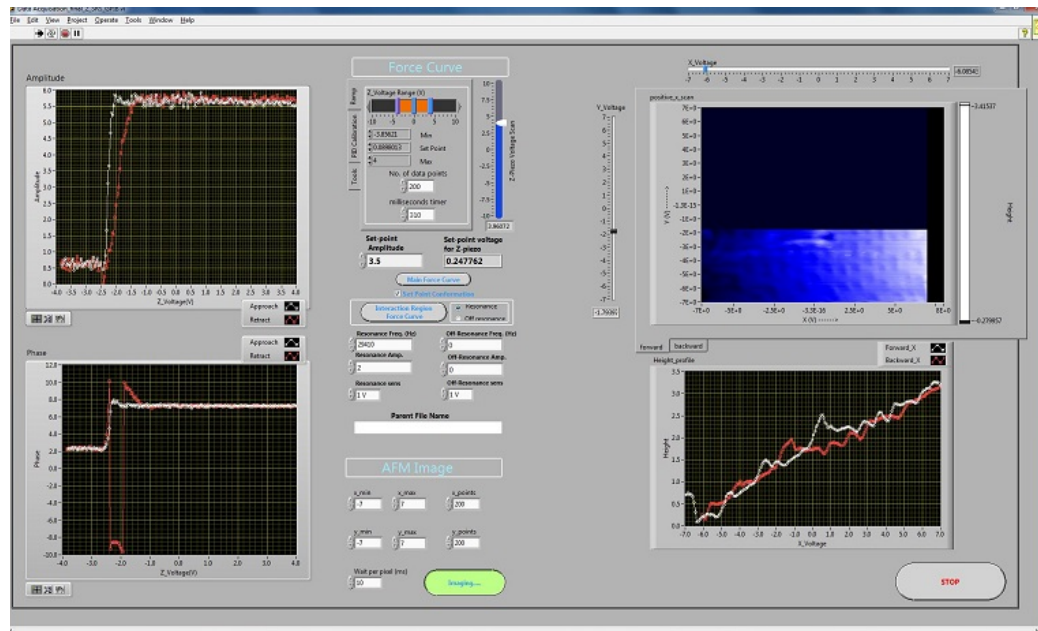


Figure 3.21: **Main data acquisition program.** This is the front panel of LabVIEW program written to do force spectroscopy and imaging with feedback

There are several other programs written for auto-approch of the tip and PI-controller calibration.

## 3.3 Calibration of Scanner piezo

The x,y calibration of the scanner piezo is done by analysing an AFM image of a known sample taken in the same set-up. The calibration sample used is a grating with  $1.6\mu\text{m}$  separation between lines. The AFM image is taken by varying the x and y voltages to scanner piezo and plotting the z voltage from PI controller which actively sets the relative tip-sample separation at a fixed force value. Then this raw image is slope-corrected using the popular open-source scanning probe image analysis software "Gwydion".

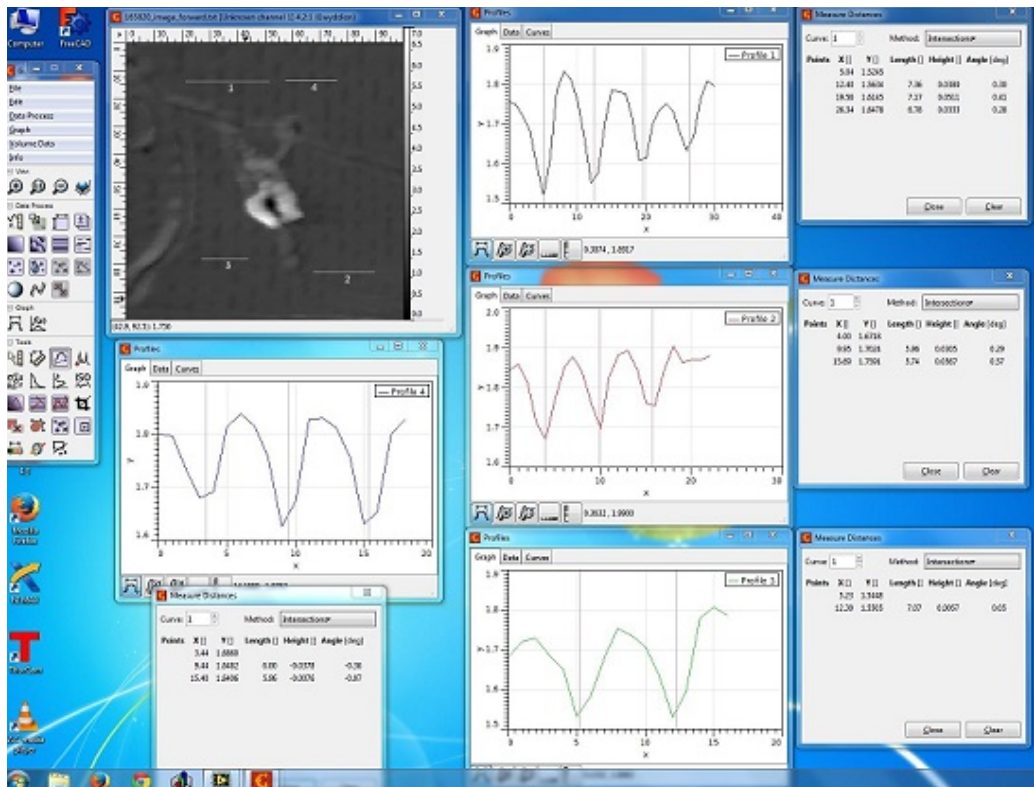


Figure 3.22: Image analysis using "Gywydion" opensource software. x, y calibration of the scanner piezo is done by analysing a known sample image taken using the set-up

From several image analysis of this sample, it is found that x sensitivity is  $131nm/V$ , y sensitivity is  $137nm/V$  and z sensitivity is  $9.5nm/V$  for the scanner piezo.

# Chapter 4

## Results

The chapter shows the main results of this project. Now instrument can work as AFM. In this chapter a few AFM images taken using the instrument is presented. In-order to compare these images, the AFM images of the same sample taken using a commercial AFM is also provided

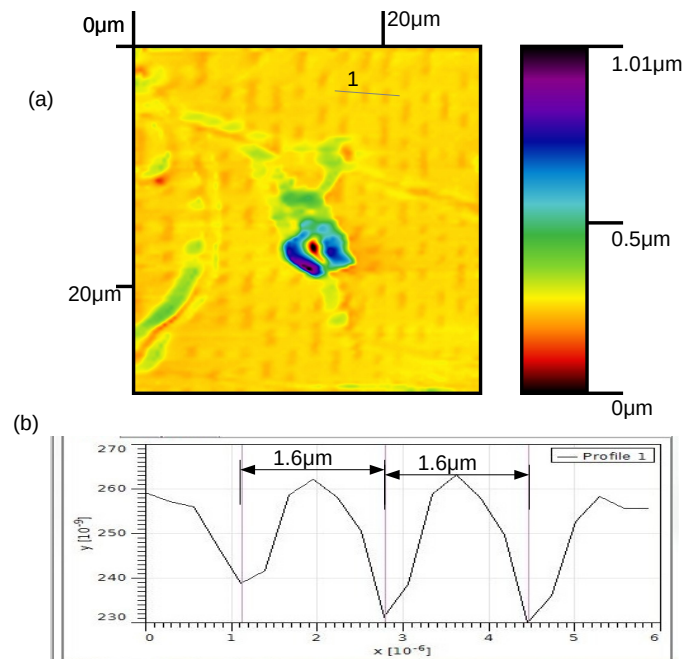


Figure 4.1: **AFM image of a grating.**(a) is the AFM image obtained from the developed instrument. (b) shows the line profile along the line 1 shown in (a) and the line separation of grating is 1.6  $\mu\text{m}$

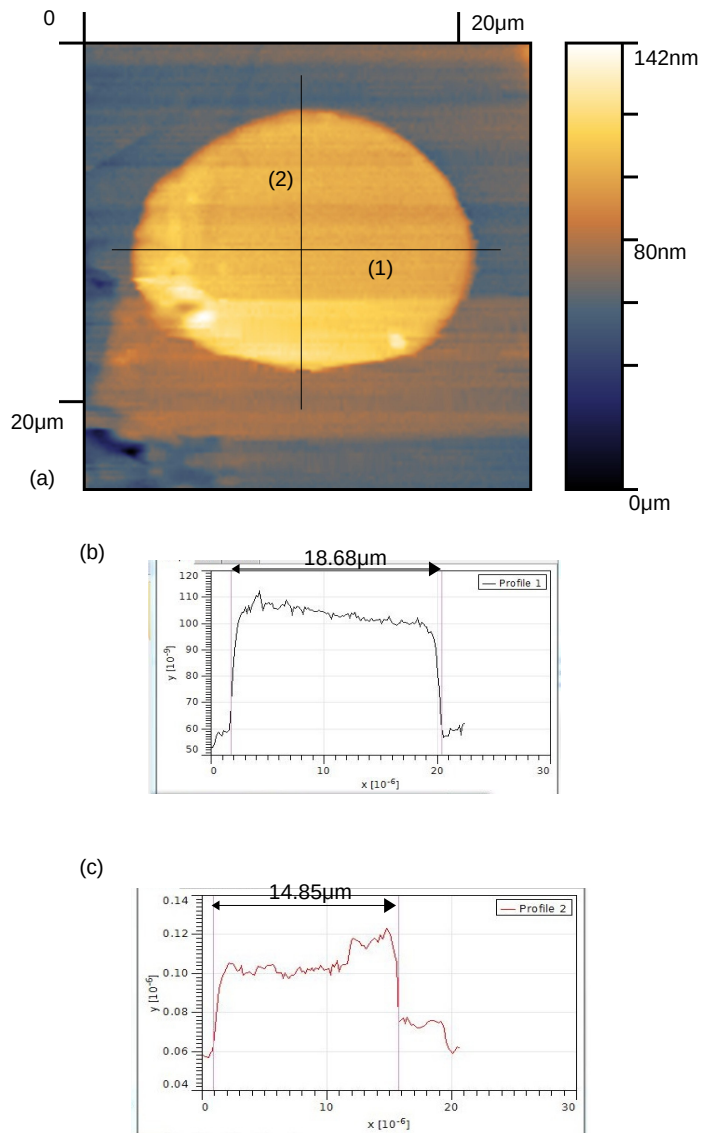


Figure 4.2: **AFM image of a circular disc.** (a) is the AFM image obtained from the developed instrument. (b) shows the line profile along the line 1 shown in (a) and the length of disc along line (1) is  $18.68\mu m$  (c) shows the line profile along the line (2) shown in (a) and the length of disc along line (2) is  $14.85\mu m$

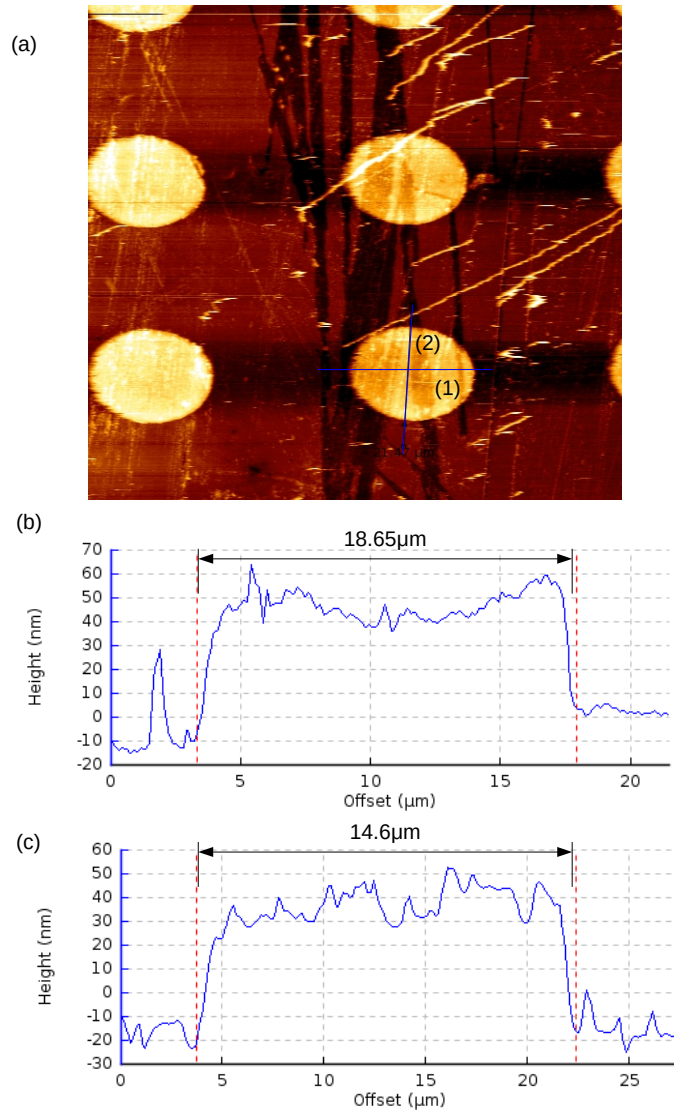


Figure 4.3: **AFM image of a circular disc.**(a) is the AFM image obtained from the commercial AFM(JPK Instruments Nanowizard II). (b) shows the line profile along the line 1 shown in (a) and the length of disc along line (1) is  $18.65\mu m$  (c) shows the line profile along the line (2) shown in (a) and the length of disc along line (2) is  $14.6\mu m$

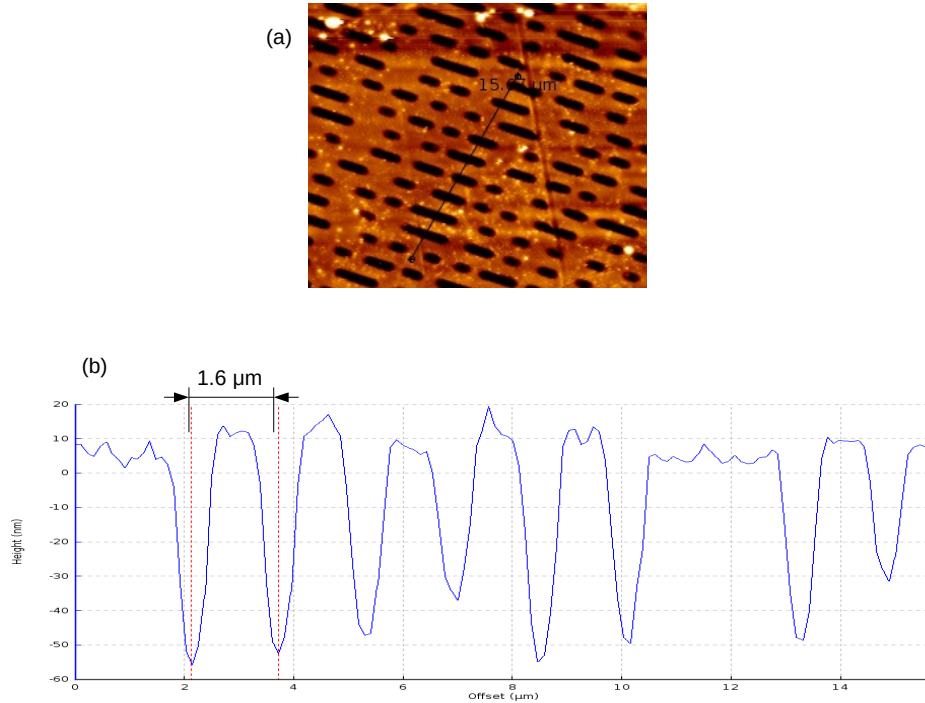


Figure 4.4: **AFM image of a grating.**(a) is the AFM image obtained from the commercial AFM(JPK Instruments Nanowizard II). (b) shows the line profile along the line 1 shown in (a) and the line separation of grating is  $1.6 \mu\text{m}$

The figure 4.1, 4.2 shows the AFM images taken. Figure 4.1 is an image of a grating which is used for calibration of distances and figure 4.1(b) shows the line profile along the line 1 shown in 4.1(a) and the line separation of grating is found out to be  $1.6 \mu\text{m}$ . The same grating is imaged using a commercial AFM for comparison (figure 4.4). Figure 4.2 is an image of a representative disc from a disc pattern fabricated over a glass slide. Same pattern is imaged using a commercial AFM to compare the image obtained. A typical amplitude and phase variations with tip-sample separation is given in figure 4.5, 4.6.

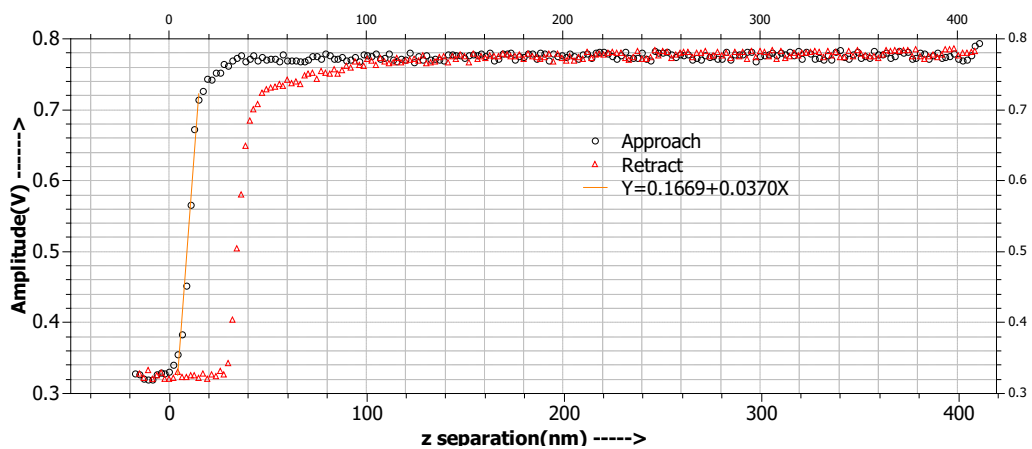


Figure 4.5: **A typical amplitude vs z-separation plot.**The plot of amplitude of tuning fork oscillation vs tip-sample separation at resonance frequency=32750Hz.

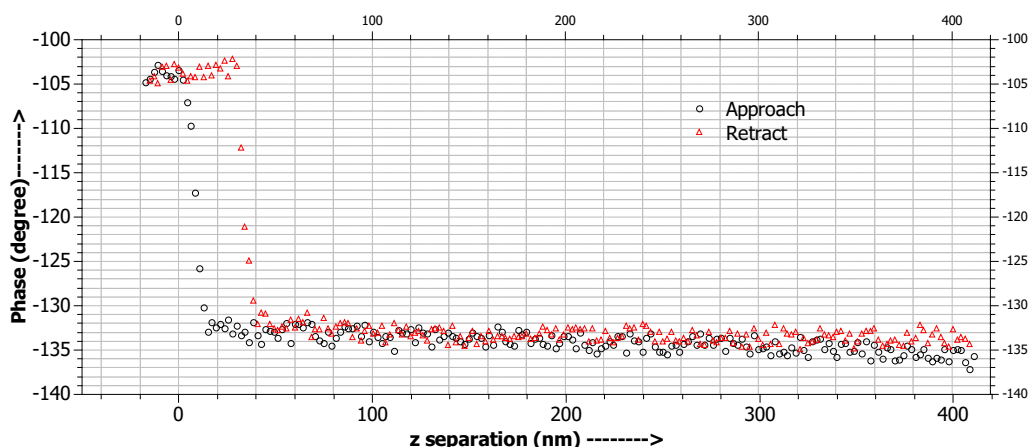


Figure 4.6: **A typical phase vs z-separation plot.**The plot of phase of tuning fork oscillation (with respect to drive) vs tip-sample separation at resonance frequency=32750Hz.



# Chapter 5

## Discussion

This chapter analyse the results and points out future direction of this project.

### 5.1 The instrument as AFM

Figure 4.1 and 4.2 shows the instrument is working as AFM. If we compare the lengths measured in the instrument and from the commercial AFM they are matching. These AFM images from the instrument shows that the electronics made for the instrument and LabVIEW program written to automate them are working as expected and PI-controller is able to keep the tip-sample height constant.

The amplitude of the drive piezo is yet to be calibrated. Once that calibration is done, using the data, amplitude and phase, shown in figure 4.5 and 4.6 we can calculate the magnitude of tip-sample interaction forces using the theory explained in chapter 2 ( 2.1).

An important peculiarity of this AFM is that, here the tip is modulated laterally so proper shear forces can be measured. While in the commercial AFM uses cantilevers, which can only immitate lateral shearing by torsional bending of cantilevers. So where ever we need to measure shear response, this AFM will give better results.

About resolution, the lateral resolution of the instrument depends on the tip size. If we use the bare optical fibre tips (figure 3.4) then the lateral resolution is around 60nm, since tip size is around 60nm. But if we use NSOM-probe fibre tips then lateral topography resolution will become 300 to 600nm (figure 3.5, 3.6).

The vertical-height resolution depends on the amplitude-separation plot (figure 4.5). From this plot we can calculate the height-sensitivity which is the

slope of the line fitted to the interaction region in amplitude- separation plot. Here it is 37mV/nm. Since the PI-controller used to keep the tip at constant height, can detect even 1mV, from this sensitivity we should be able to detect 0.1nm easily. Such a good tip-sample distance control is much needed for the instrument to work as NSOM.

## 5.2 The instrument as NSOM

It took some time to get the FIB facility to make the optical probes. As the FIB facility was not available in IISER Pune when this thesis work is done, had to search for FIB facility and finally got the FIB slot from IIT Mumbai (OIM and Texture Lab). Now the NSOM-fibre probes are ready (figure 3.6) and a PMT-cap is made to attach the fibre to PMT. Within one week fibre tip can be loaded with PMT in the set-up. The results of NSOM will be put up in the thesis presentation.

## 5.3 In Future

As discussed in introduction chapter, the main motivation to build this instrument is to study nano-confined water. Many experiments can be done on nano-confined water. One is diffusion measurement of a fluorescent particle through the confined water. Another one is that checking for critical opalescence on confinement. These experiments will be the first attempt to probe nano-confined water optically.

Application of this instrument is not just limited to studying nano-confined water. Using this instrument one can study the shear properties of bilayers along with it's optical image or can map the optical light intensity on different nano-wire geometries due to surface plasmons.

## References

- [1] E.H.Synge, A suggested model for extending microscopic resolution into the ultra-microscopic region, *Phil. Mag.* 6 (1928) 356–362.
- [2] J. A. O’KEEFE, Resolving power of visible light, *J. Opt. Soc. Am.* 46 (5) (1956) 359–359. doi:10.1364/JOSA.46.000359.  
URL <http://www.opticsinfobase.org/abstract.cfm?URI=josa-46-5-359>
- [3] E. A. Ash, G. Nicholls, Super-resolution aperture scanning microscope, *Nature* 237 (1972) 510–513.
- [4] R. Young, J. Ward, F. Scire, The topografiner: An instrument for measuring surface microtopography, *Review of Scientific Instruments* 43 (7).
- [5] G. Binnig, H. Rohrer, C. Gerber, E. Weibel, Surface studies by scanning tunneling microscopy, *Phys. Rev. Lett.* 49 (1982) 57–61. doi:10.1103/PhysRevLett.49.57.  
URL <http://link.aps.org/doi/10.1103/PhysRevLett.49.57>
- [6] D. W. Pohl, W. Denk, M. Lanz, Optical stethoscopy: Image recording with resolution  $\lambda/20$ , *Applied Physics Letters* 44 (7).
- [7] A. Lewis, M. Isaacson, A. Harootunian, A. Muray, Development of a 500 Å spatial resolution light microscope: I. light is efficiently transmitted through  $\lambda/16$  diameter apertures, *Ultramicroscopy* 13 (3) (1984) 227 – 231. doi:[http://dx.doi.org/10.1016/0304-3991\(84\)90201-8](http://dx.doi.org/10.1016/0304-3991(84)90201-8).  
URL <http://www.sciencedirect.com/science/article/pii/0304399184902018>
- [8] G. Binnig, C. F. Quate, C. Gerber, Atomic force microscope, *Phys. Rev. Lett.* 56 (1986) 930–933. doi:10.1103/PhysRevLett.56.930.  
URL <http://link.aps.org/doi/10.1103/PhysRevLett.56.930>

- [9] E. Betzig, J. K. Trautman, R. Wolfe, E. M. Gyorgy, P. L. Finn, M. H. Kryder, C.-H. Chang, Near-field magneto-optics and high density data storage, *Applied Physics Letters* 61 (2).
- [10] E. Betzig, S. G. Grubb, R. J. Chichester, D. J. DiGiovanni, J. S. Weiner, Fiber laser probe for near-field scanning optical microscopy, *Applied Physics Letters* 63 (26).
- [11] R. D. Grober, T. D. Harris, J. K. Trautman, E. Betzig, W. Wegscheider, L. Pfeiffer, K. West, Optical spectroscopy of a gaas/algaas quantum wire structure using near-field scanning optical microscopy, *Applied Physics Letters* 64 (11).
- [12] J. Klein, E. Kumacheva, Confinement-induced phase transitions in simple liquids, *Science* 269 (5225) (1995) 816–819. [arXiv: http://www.sciencemag.org/content/269/5225/816.full.pdf](http://www.sciencemag.org/content/269/5225/816.full.pdf), [doi:10.1126/science.269.5225.816](https://doi.org/10.1126/science.269.5225.816).  
URL <http://www.sciencemag.org/content/269/5225/816.abstract>
- [13] S. Granick, Motions and relaxations of confined liquids, *Science* 253 (5026) (1991) 1374–1379.
- [14] P. L. . J. K. Uri Raviv, Fluidity of water confined to subnanometre films, *Nature* 413 (2001) 51–54.
- [15] S. H. Khan, G. Matei, S. Patil, P. M. Hoffmann, Dynamic solidification in nanoconfined water films, *Phys. Rev. Lett.* 105 (2010) 106101. [doi:10.1103/PhysRevLett.105.106101](https://doi.org/10.1103/PhysRevLett.105.106101).  
URL <http://link.aps.org/doi/10.1103/PhysRevLett.105.106101>
- [16] K. Kapoor, Amandeep, S. Patil, Viscoelasticity and shear thinning of nanoconfined water, *Phys. Rev. E* 89 (2014) 013004. [doi:10.1103/PhysRevE.89.013004](https://doi.org/10.1103/PhysRevE.89.013004).  
URL <http://link.aps.org/doi/10.1103/PhysRevE.89.013004>
- [17] S. Granick, S. C. Bae, S. Kumar, C. Yu, Confined liquid controversies near closure?, *Physics* 3 (2010) 73. [doi:10.1103/Physics.3.73](https://doi.org/10.1103/Physics.3.73).  
URL <http://link.aps.org/doi/10.1103/Physics.3.73>
- [18] K. Kapoor, V. Kanawade, V. Shukla, S. Patil, A new tuning fork-based instrument for oscillatory shear rheology of nano-confined liquids, *Review of Scientific Instruments* 84 (2) (2013) –. [doi:http://dx.doi.org/10.1063/1.4789431](https://doi.org/10.1063/1.4789431).

- URL <http://scitation.aip.org/content/aip/journal/rsi/84/2/10.1063/1.4789431>
- [19] F. J. Giessibl, Atomic resolution on si(111)-(7 $\times$ 7) by noncontact atomic force microscopy with a force sensor based on a quartz tuning fork, *Applied Physics Letters* 76 (11).
- [20] M. Lee, J. Jahng, K. Kim, W. Jhe, Quantitative atomic force measurement with a quartz tuning fork, *Applied Physics Letters* 91 (2) (2007) –. doi:<http://dx.doi.org/10.1063/1.2756125>.  
URL <http://scitation.aip.org/content/aip/journal/apl/91/2/10.1063/1.2756125>
- [21] F. J. Giessibl, High-speed force sensor for force microscopy and profilometry utilizing a quartz tuning fork, *Applied Physics Letters* 73 (26) (1998) 3956–3958. doi:<http://dx.doi.org/10.1063/1.122948>.  
URL <http://scitation.aip.org/content/aip/journal/apl/73/26/10.1063/1.122948>
- [22] A. Lipson, S. Lipson, H. Lipson, *Optical Physics*, Cambridge University Press, 2010.
- [23] L. Novotny, B. Hecht, *Principles of Nano-Optics*, Cambridge University Press, 2006.
- [24] J. A. Veerman, A. M. Otter, L. Kuipers, N. F. van Hulst, High definition aperture probes for near-field optical microscopy fabricated by focused ion beam milling, *Applied Physics Letters* 72 (24) (1998) 3115–3117. doi:<http://dx.doi.org/10.1063/1.121564>.  
URL <http://scitation.aip.org/content/aip/journal/apl/72/24/10.1063/1.121564>
- [25] S. Patil, G. Matei, H. Dong, P. M. Hoffmann, M. Karaköse, A. Oral, A highly sensitive atomic force microscope for linear measurements of molecular forces in liquids, *Review of Scientific Instruments* 76 (10) (2005) –. doi:<http://dx.doi.org/10.1063/1.2083147>.  
URL <http://scitation.aip.org/content/aip/journal/rsi/76/10/10.1063/1.2083147>